Revealing two-stage phase transition process in defective $KTaO_3$ under inelastic interactions

D. Iancu[a,d], E. Zarkadoula[b], M. D. Mihai[a], C. Burducea[a], I. Burducea[a], M. Straticiuc[a], Y. Zhang[b,c], W. J. Weber[c**] and G. Velişa[a*]

[a]Horia Hulubei National Institute for Physics and Nuclear Engineering, Măgurele, IF 077125, Romania
[b]Materials Science and Technology Division, Oak Ridge National Laboratory, Oak Ridge, TN 37831, USA
[c]Department of Materials Science & Engineering, University of Tennessee, Knoxville, TN 37996, USA
[d]University of Bucharest, Faculty of Physics, Măgurele, IF 077125, Romania

Abstract

The interactions of ions with defective $KTaO_3$ has been studied by irradiating pre-damaged single crystal $KTaO_3$ with 5 MeV C, 7 MeV Si and 12 MeV O ions at 300 K. By exploring these processes in $KTaO_3$, the results show that, for a pre-damaged fractional disorder level of 0.3 and inelastic electronic energy loss, $S_e \geq 4.65$ keV/nm (7 MeV Si ions), the synergistic interaction of S_e with defects enables amorphous ion track creation. At lower values of S_e (5 MeV C and 12 MeV O), minor increases in disorder are observed initially over a region of depth at an ion fluence of 10 ions/nm^2, which may be due to dissolution of pre-existing interstitial or amorphous clusters; however, with further increase in ion fluence, a transition from irradiation-induced disorder production to ionization-induced damage recovery processes, not previously reported in $KTaO_3$, is observed.

Keywords: perovskite, ion channeling, molecular dynamics, ion-induced annealing, two-stage process
* Corresponding author. Horia Hulubei National Institute for Physics and Nuclear Engineering, Măgurele, IF 077125, Romania
E-mail addresses: gihan.velisa@nipne.ro (Gihan Velişa), Tel: +4 0723-933-922

** Corresponding author. Materials Science and Engineering, University of Tennessee, Knoxville, TN 37006, USA.
E-mail addresses: wjweber@utk.edu (William J. Weber), Tel: +1 865-974-0415

Interest in ion beam modification of potassium tantalate ($KTaO_3$) properties has rapidly risen in the last decade, fueled by the tunability of its electronic [1–3] and optical [4–7] properties through defect engineering [8]. A recent review [8] has further validated that the creation of new functionalities in $KTaO_3$ through ion implantation (doping) [9] or irradiation (nanoscale phase transformations and defect creation) [6] requires atomic-level control of microstructural modifications, which is challenging to achieve if the material response to the combined consequences of electronic and nuclear energy dissipation is not well understood [10–12]. The effect of nuclear energy loss (S_n) from irradiation with low-energy ions on the behavior of virgin $KTaO_3$ can be predicted a priori because it is reasonably well understood [13–15]. Researchers have reported [15] that the dependence of low-energy irradiation-induced disorder on ion fluence is characterized by a sigmoidal behavior that leads to a fully amorphous state, through a defect-stimulated mechanism [15], at irradiation temperatures below a critical amorphization temperature.

Experimental and theoretical studies on the response of virgin $KTaO_3$ to the dissipation of electronic energy loss (S_e) to the lattice under high-energy ion irradiation have shown that highly ionizing charged-particles with S_e exceeding the critical threshold value ($S_e^{th} \geq 10.81$ keV/nm), can give rise to the generation of individual amorphous ion tracks [16,17]; however, measurable effects of ionization energy dissipation on damage production have not been reported in pristine $KTaO_3$ for ions with values of S_e below 10.81 keV/nm [18]. The impact of S_e dissipation on the behavior of pre-damaged material are, on the other hand, more difficult to predict a priori because previous studies have demonstrated that the interplay between S_e dissipation and already-existing lattice disorder created by ions in the high S_n regime can either enhance damage accumulation/amorphization (synergistic effect) or can induce damage annealing (competitive effect) [11]. For example, our previous study [18] has revealed that irradiation of pre-damaged $KTaO_3$ with ionizing ions having S_e values above

specific threshold values, S_e^{th}, induces the creation of ion tracks due to synergistic coupling between ionization energy dissipation and already-existing damage. This work also concluded that the values of S_e^{th} decrease with increasing amount of initially induced disorder (f_0). Finally, this previous study [18] revealed that synergistic coupling is not operative for f_0 = 0.08 and a value of $S_e \sim 6.16$ keV/nm; however, no clear evidence for the existence of a competitive effect was observed. In the work presented here, the consequences of ionizing particles on damage evolution in defective $KTaO_3$ are investigated using ions with S_e values below the subthreshold regime for ion track formation previously determined ($S_e^{th} \approx 5.77$ keV/nm).

Four monocrystalline $KTaO_3$ samples (https://www.alineason.com/) were initially irradiated with 2.0 MeV Au ions several degrees away from the zone axis at 300 K to ion fluences of 1.1×10^{13}, and 1.8×10^{13} ions/cm^2, respectively. The average particle flux during Au ion irradiations was $\sim 1.6 \times 10^{10}$ cm^{-2}s^{-1}. In the next step of the experimental procedure, both virgin (undamaged) and defective $KTaO_3$ crystals were sequentially irradiated at 300 K to various ion fluences with 5 MeV C, 7 MeV Si and 12 MeV O ions. The average particle flux during the C and O ion irradiations was 1.1×10^{11} and 5×10^{10} cm^{-2}s^{-1}, respectively. The S_e and S_n values were calculated via the Stopping and Range of Ions in Matter (SRIM-v2006.02) code [19,20], using the density given by the manufacturer (7.03 g/cm^3), and these predicted values are given in Table 1. After each irradiation sequence, *ex-situ* Rutherford backscattering spectrometry in channeling geometry (RBS/C) was conducted, using 2 MeV alpha particles, to characterize and quantify the evolution of the damage state as a result of irradiation with highly ionizing particles. Ion irradiations and *ex-situ* RBS/C were completed using the instrumentation available at the second and first beam line end-stations, respectively, of the 3 MV accelerator located at IFIN-HH, Magurele, Romania [21,22]. Further, to model the inelastic interactions of ions with defective $KTaO_3$, and to provide new

insights into the ion channeling results, molecular dynamics (MD) simulations in conjunction with the inelastic thermal spike model (i-TS) were executed using the DL_POLY MD package [23]. The modeling details are provided in the supplementary material.

Table 1: SRIM-depicted S_e, S_n, and ratio S_e/S_n at the Au-induced damage peak (160 nm) in $KTaO_3$ for indicated ion species. The corresponding local damage dose in displacements per atom (dpa) for the indicated ion fluences is also included.

Ion/energy	S_e (keV/nm)	S_n (keV/nm)	S_e/S_n	dpa @ 160 nm
5 MeV C	2.17	0.004	542	0.046 (70 ions/nm^2)
7 MeV Si	4.65	0.03	130	0.0001 (0.2 ions/nm^2)
12 MeV O	3.03	0.003	1010	0.039 (60 ions/nm^2)

Analysis of each RBS/C spectra was performed utilizing an iterative approach [24] in order to ascertain the depth profile of relative Ta disorder for the defective $KTaO_3$ prior to and after sequential ionizing irradiation. Based on this analysis, the relative disorder is equal to 1.0 for an amorphous or random state; whereas for the virgin crystal (undamaged), it is assumed to be 0. Here, the dependence of relative disorder on ion fluence (ions/nm^2 = 10^{14} ions/cm^2) is reported.

Irradiation with Au ions to an ion fluence of 0.11 ions/nm^2 creates a pre-damaged state with an initial maximum level of fraction disorder (f_0) of 0.35 on the Ta sublattice, as shown in Fig. 1(a). Subsequent irradiation with 7 MeV Si ions results in accelerated accumulation of disorder, as clearly indicated in Fig. 1(a) by the rise of relative disorder across the whole pre-damaged layer with increasing Si fluence. Given the high and very small values for S_e and S_n for 7 MeV Si ions, respectively, across the pre-damaged layer, this accelerated damage accumulation is ascribed primarily to the creation of continuous (uninterrupted) or discontinuous (fragmented) amorphous ion tracks along individual ion trajectories [25], triggered by the synergistic coupling between S_e and pre-existing defects [18,26,27]; while disorder induced by S_n should be negligible across the pre-damaged layer. Here one should

note that for the highest Si fluence (0.2 ions/nm^2) used in the current study, the corresponding dpa value at the Au-induced damage peak (160 nm) is about 0.001 dpa. Our recent studies [16–18,27] have demonstrated that 18 MeV Si and 21 MeV Ni ions produce ion tracks in pre-damaged $KTaO_3$ with f_0 of 0.3 at S_e values above 6.16 keV/nm [18]. These same studies have used the direct-impact model [28,29] to determine the amorphous cross-section (σ_a) associated with cylindrical track generation in defective $KTaO_3$, and this model is used here to derive σ_a from the data in Fig. 1(b). As discussed in detail elsewhere [18], the amorphous fraction, f_a, at the damage peak from direct-impact amorphization can be obtained by:

$$f_a = 1 - (1 - f_0) \times \exp(-\sigma_a \times \Phi), \quad (1)$$

where Φ is the fluence of the ionizing ions, and as mentioned above f_0 is the initial disorder fraction in pre-damaged $KTaO_3$. A fit of Eq. (1) to the data in Fig. 1 (b) yields $\sigma_a = 3.69 \pm 0.07$ nm^2 and average track diameter, d = 2.17 ± 0.2 nm, for pre-damaged $KTaO_3$ ($f_0 = 0.33$) and sequentially irradiated with 7 MeV Si ions. Based on MD simulations for the case of 7 MeV Si ions, the dissipation of S_e generates a thermal spike sufficient to create an ion track within the defective layer (see Fig. 1(c)). The inset of Fig. 1 (c) illustrates a cross section of the MD box (20 nm × 20 nm) where an amorphous ion track (d = 3.4 ± 0.1 nm) is formed from the thermal spike of a 7 MeV Si ion. Here, one should note that even if the samples were not cracked (see Fig. S2), quantifying continuous or discontinuous tracks with diameters ≤ 2.2 nm in samples containing high levels of already-existing damage, as in this study, is difficult through TEM analysis [18,30]. The track cross sections determined for 7 MeV Si-irradiated defective $KTaO_3$ are plotted vs. S_e in Fig. 1(d), together with previous results for 18 MeV Si [18], 21 MeV Ni [27] and 91.6 MeV Xe [18] ion irradiations of pre-damaged KTO_3 under identical irradiation conditions. The curve in Fig. 1(d) is a polynomial fit to the data. From the

extrapolation of the σ_a dependence on S_e, the threshold value for track formation, due to ionizing irradiation of defective $KTaO_3$ with a maximum initial disorder fraction $f_0 = 0.3$, is $S_e^{th} = 4.83$ keV/nm. This value is smaller than the previously-predicted threshold value of 5.77 keV/nm for the same initial disorder level [18].

To understand the evolution of already-damaged $KTaO_3$ to lower values of S_e, we further analyze the response of $KTaO_3$ pre-damaged with Au ions to a fluence of 0.18 ions/nm^2 and subsequently irradiated with 5 MeV C and 12 MeV O ions. As shown in Fig. 2 (see black lines), the irradiation of $KTaO_3$ with 2 MeV Au to a fluence of 0.18 ions/nm^2 results in a higher initial relative peak disorder ($f_0 \sim 0.8$). Subsequent irradiation with either C or O ions to a fluence of 10 ions/nm^2 slightly increases the peak disorder level to 0.86 and 0.96, respectively; however, in the case of O ions, the width of the damage profile decreases, indicating some annealing at lower levels of disorder. Note that in the case of C ions, the slight increase may be within the experimental uncertainty. With further irradiation to higher ion fluences, the peak disorder level and the width of the disorder profile both decrease with increasing ion fluence for C and O ions. For both ions, there appears to be a transitory stage at fluences up to 10 ions/nm^2, where the level of disorder in the peak region increases. This can be accompanied by annealing at lower levels of disorder (e.g., 12 MeV O ions), resulting in a decrease in width of the disorder profile. At these high levels of disorder (0.5 to 0.8), the damage consists primarily of interstitial clusters and nanoscale amorphous domains, and the irradiation-induced dissociation of these extended defects into point defects and smaller clusters could account for the slight increase in interstitial disorder observed in the region of the disorder peak. These point defects and smaller clusters would be more susceptible to annealing, similar to the annealing that results in the decrease in width of the disorder profile. The local irradiation-induced dissociation of extended defects is likely due from ejection of atoms from the defects due to atomic displacement processes induced by S_e or S_n (or both),

which is consistent with the uniform disorder production with depth in the virgin crystal for both C and O ions, as shown in Fig. S1(c). This effect is usually called in-cascade damage production. However, further work is needed to identify the processes associated with the slight increase in disorder. At higher fluences, damage annealing clearly dominates over damage production for both C and O ions. Similar behavior is also observed for lower initial f_0 (~0.35) on the Ta sublattice (see Fig. S1 in the supplementary file).

It has been shown previously that the recovery cross section (σ_r) associated with ionization-induced recovery process in pre-damaged $SrTiO_3$, can be determined by fitting a simple exponential function to the dependence of the normalized recovery of relative peak disorder (f/f_0) on ion fluence [31]. Having in mind that, in the transitory stage, the relative peak disorder of the pre-damaged samples increases somewhat following irradiation with C and O ions to fluences of 10 ions/nm^2, we will consider these higher disorder levels (0.86 and 0.96, respectively, for C and O ions) as new f_0 values in the analysis of annealing. In the analysis of annealing behavior, we integrate and normalize the relative disorder profiles to determine a relative areal density of damage (A/A_0) and evaluate the dependence on fluence, because under current experimental conditions, the reduction of disorder level is accompanied by the decrease in width of the disorder profiles with increasing ion fluence (see Fig. 2). This representation also follows the same exponential decrease with rising fluence of ionizing ions, ϕ, depicted by the formula:

$$A/A_0 = 1 - A_r/A_0 \times [1 - \exp(-\sigma_r \times \Phi)], \quad (2)$$

where A_r/A_0 represents the recoverable fraction of disorder. Since the recovery data seem to fall on a single curve, only a single fit using Eq. (2) to the data in Fig. 3 is performed. This fit yields a recovery cross section of $\sigma_r = 0.0209$ nm^2 for both C and O ions. The cross-sections

obtained by fitting a limited number of data, as in the present study, should be reported with large error bar (i.e., 50%) [32].

To understand the effect of S_e in the subthreshold regime for ion track formation, the spatial evolution of lattice temperature in defective layer of $KTaO_3$ irradiated with ionizing ions was simulated using MD simulations in conjunction with the i-TS model. The maximum temperature profiles (at a time of 30 fs) are provided in Fig. 4, along with the equivalent curve for 7 MeV Si ions. The highest lattice temperature is around 18,750 K for 7 MeV Si ions, and this temperature should be enough to trigger the occurrence of a molten zone, leading to the formation of ion track. In contrast, for C and O ions, the simulations show neither track formation nor defect annealing, for irradiation with four ions. This means that the ionization-induced annealing processes in $KTaO_3$ occurring at high ion fluences are not easily captured using atomistic modeling, which is consistent with the very small recovery cross section measured experimentally and the high fluences needed to induce annealing. In contrast, MD simulations have captured the ionization-induced annealing due 12 MeV O ions in $SrTiO_3$ [31], where the recovery cross section (0.38 nm^2) is a factor of 180 times larger. Based on previous work [31], we estimate that up to 400 individual ion events in a confined volume may be required to simulate the recovery occurring in $KTaO_3$. Deficiencies of the empirical potentials to describe atomic diffusion processes may also inhibit recovery simulations, but is beyond the scope of the current work.

The consequences of ionizing particles on damage evolution in defective $KTaO_3$ has been investigated using ions with electronic energy transfer (S_e) values below the previously determined threshold for ion track production in pre-damaged $KTaO_3$. For Si ions, the RBS/C clearly shows that the synergistic effect is active and induces the formation of small ion tracks, which is well in line with MD simulations. For C and O ions, RBS/C measurements reveal a competitive two-stage phase transition process that leads to damage recovery process,

not previously reported in $KTaO_3$. Further *in-situ* TEM analysis in conjunction with MD simulations [33] will be necessary to enable new mechanistic insights into the atomic nature of the observed transition in $KTaO_3$.

Acknowledgements

This work was supported by a grant of the Romanian Ministry of Education and Research, CNCS—UEFISCDI, project number PN-III-P4-IDPCE2020- 1379, within PNCDI III. The contributions of Y. Zhang and W. J. Weber to this work were supported by the National Science Foundation under Grant No. DMR-2104228.

References

[1] S. Harashima, C. Bell, M. Kim, T. Yajima, Y. Hikita, H.Y. Hwang, Phys. Rev. B 88 (2013) 085102.

[2] R. Tomar, N. Wadehra, S. Kumar, A. Venkatesan, D.D. Sarma, D. Maryenko, S. Chakraverty, J. Appl. Phys. 126 (2019) 035303.

[3] S.K. Ojha, S.K. Gogoi, P. Mandal, S.D. Kaushik, J.W. Freeland, M. Jain, S. Middey, Phys. Rev. B 103 (2021) 085120.

[4] V. V. Laguta, M.D. Glinchuk, I.P. Bykov, A. Cremona, P. Galinetto, E. Giulotto, L. Jastrabik, J. Rosa, J. Appl. Phys. 93 (2003) 6056.

[5] Y. Liu, X. Han, Q. Huang, M.L. Crespillo, P. Liu, E. Zarkadoula, X. Wang, J. Mater. Sci. Technol. 90 (2021) 95–107.

[6] X. Han, Y. Liu, Q. Huang, M.L. Crespillo, P. Liu, X. Wang, J. Phys. D. Appl. Phys. 53 (2020) 105304.

[7] J.Y.C. Wong, L. Zhang, G. Kakarantzas, P.D. Townsend, P.J. Chandler, L.A. Boatner, J. Appl. Phys. 71 (1992) 49–52.

[8] A. Gupta, H. Silotia, A. Kumari, M. Dumen, S. Goyal, R. Tomar, N. Wadehra, P. Ayyub, S. Chakraverty, Adv. Mater. (2022) 2106481.

[9] K. Ueno, S. Nakamura, H. Shimotani, H.T. Yuan, N. Kimura, T. Nojima, H. Aoki, Y. Iwasa, M. Kawasaki, Nat. Nanotechnol. 6 (2011) 408–412.

[10] W. Wesch, E. Wendler, Ion Beam Modification of Solids : Ion-Solid Interaction and Radiation Damage, 2016.

[11] Y. Zhang, W.J. Weber, Appl. Phys. Rev. 7 (2020) 041307.

[12] X. Han, Q. Huang, M.L. Crespillo, E. Zarkadoula, Y. Liu, X. Wang, P. Liu, J. Mater. Sci. Technol. 116 (2022) 30–40.

[13] A. Meldrum, L.A. Boatner, R.. Ewing, Nucl. Instruments Methods Phys. Res. Sect. B Beam Interact. with Mater. Atoms 141 (1998) 347–352.

[14] A. Meldrum, L.A. Boatner, W.J. Weber, R.C. Ewing, J. Nucl. Mater. 300 (2002) 242–254.

[15] G. Velişa, E. Wendler, L.-L. Wang, Y. Zhang, W.J. Weber, J. Mater. Sci. 54 (2019) 149–158.

[16] E. Zarkadoula, K. Jin, Y. Zhang, W.J. Weber, AIP Adv. 7 (2017) 1–8.

[17] E. Zarkadoula, Y. Zhang, W.J. Weber, AIP Adv. 10 (2020) 015019.

[18] G. Velişa, E. Zarkadoula, D. Iancu, M.D. Mihai, C. Grygiel, I. Monnet, B. Kombaiah, Y. Zhang, W.J. Weber, J. Phys. D. Appl. Phys. 54 (2021) 375302.

[19] W.J. Weber, Y. Zhang, Curr. Opin. Solid State Mater. Sci. 23 (2019) 100757.

[20] J.F. Ziegler, J.P. Biersack, in: Treatise Heavy-Ion Sci., Springer US, Boston, MA, 1985, pp. 93–129.

[21] I. Burducea, M. Straticiuc, D.G. Ghiță, D.V. Moșu, C.I. Călinescu, N.C. Podaru, D.J.W. Mous, I. Ursu, N.V. Zamfir, Nucl. Instruments Methods Phys. Res. Sect. B Beam Interact. with Mater. Atoms 359 (2015) 12–19.

[22] G. Velişa, R.F. Andrei, I. Burducea, A. Enciu, D. Iancu, D.A. Mirea, A. Spiridon, M. Straticiuc, Eur. Phys. J. Plus 2021 13611 136 (2021) 1–13.

[23] I.T. Todorov, W. Smith, K. Trachenko, M.T. Dove, J. Mater. Chem. 16 (2006) 1911–1918.

[24] Y. Zhang, J. Lian, Z. Zhu, W.D. Bennett, L.V. Saraf, J.L. Rausch, C.A. Hendricks, R.C. Ewing, W.J. Weber, J. Nucl. Mater. 389 (2009) 303–310.

[25] M. Lang, F. Djurabekova, N. Medvedev, M. Toulemonde, C. Trautmann, in: Ref. Modul. Mater. Sci. Mater. Eng., Elsevier, 2020.

[26] H. Xue, E. Zarkadoula, P. Liu, K. Jin, Y. Zhang, W.J. Weber, Acta Mater. 127 (2017)

400–406.
[27] K. Jin, Y. Zhang, W.J. Weber, Mater. Res. Lett. 6 (2018) 531–536.
[28] J.F. Gibbons, Proc. IEEE 60 (1972) 1062–1096.
[29] W.J. Weber, Nucl. Instruments Methods Phys. Res. Sect. B Beam Interact. with Mater. Atoms 166–167 (2000) 98–106.
[30] L. Thomé, in: Springer Ser. Surf. Sci., Springer Verlag, 2016, pp. 321–363.
[31] W.J. Weber, H. Xue, E. Zarkadoula, Y. Zhang, Scr. Mater. 173 (2019) 154–157.
[32] A. Debelle, M. Backman, L. Thomé, K. Nordlund, F. Djurabekova, W.J. Weber, I. Monnet, O.H. Pakarinen, F. Garrido, F. Paumier, Nucl. Instruments Methods Phys. Res. Sect. B Beam Interact. with Mater. Atoms 326 (2014) 326–331.
[33] H. Zhu, M. Qin, R. Aughterson, T. Wei, G. Lumpkin, Y. Ma, H. Li, Acta Mater. 172 (2019) 72–83.

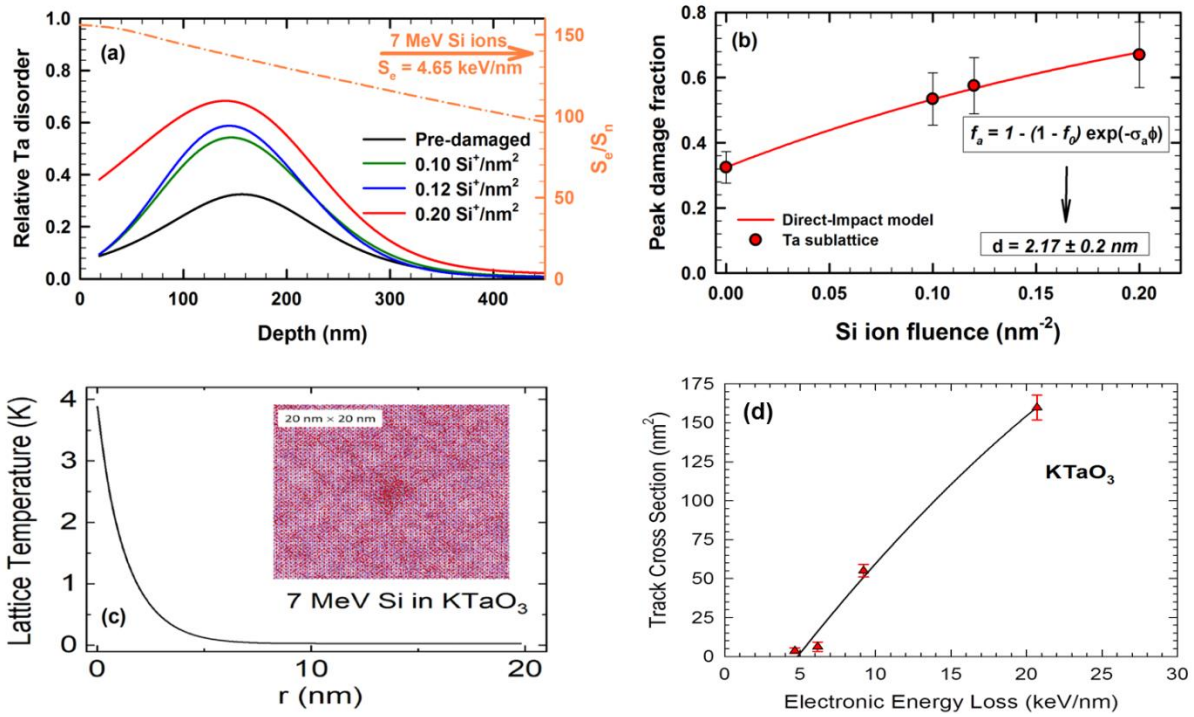

Fig.1. (a) Relative Ta disorder profiles for pre-damaged $KTaO_3$ with a maximum initial disorder fraction f_0 = 0.3 and subsequently irradiated with 7 MeV Si ions. Note that the parameters (ion energy, fluence and S_e) are indicated in the figure. Also superimposed are the SRIM-derived S_e/S_n ratios (dash lines). (b) Increase in peak damage fraction (i.e., at depth of 160 nm) on the Ta sublattice with increasing 7 MeV Si ion fluence in the defective $KTaO_3$. The curve fit shown of the DI model (Eq. 1) yields the value of σ_a directly: 3.69 ± 0.07 nm^2. (c) Radial profile of the calculated lattice temperature induced by the inelastic thermal spike from a 7 MeV Si ion in $KTaO_3$ containing 30 % Frenkel pairs. The inset shows a cross section of the MD box, with size 20 nm × 20 nm, where an amorphous ion track with a diameter of 3.4 ± 0.1 nm has formed due to the inelastic thermal spike. (d) Track cross section vs. S_e in $KTaO_3$ containing a maximum initial peak disorder level f_0 = 0.3.

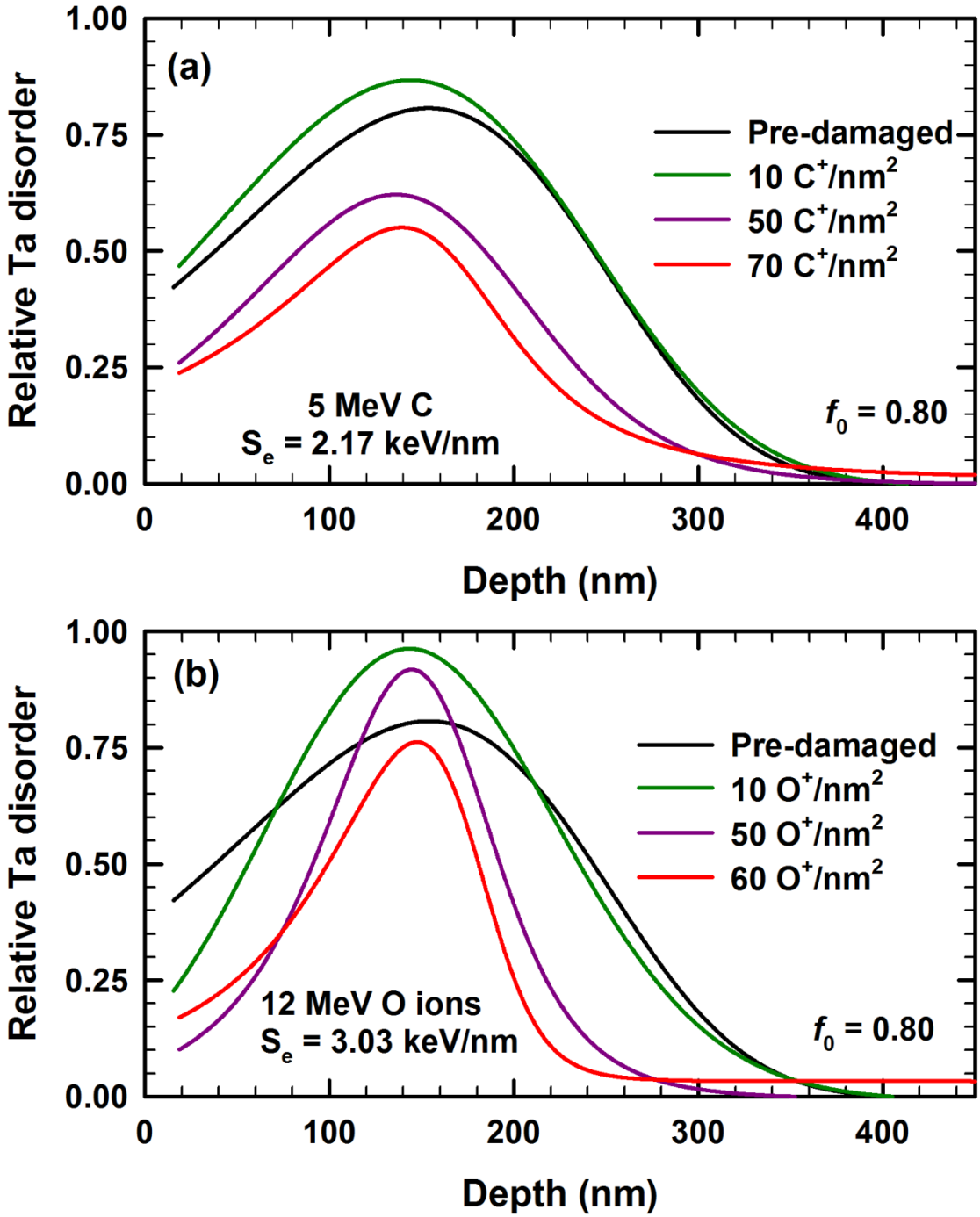

Fig. 2. Change in relative Ta disorder profiles in defective $KTaO_3$ containing a maximum initial peak disorder fraction $f_0 = 0.8$ due to subsequent irradiation with: (a) 5 MeV C ions and (b) 12 MeV O ions.

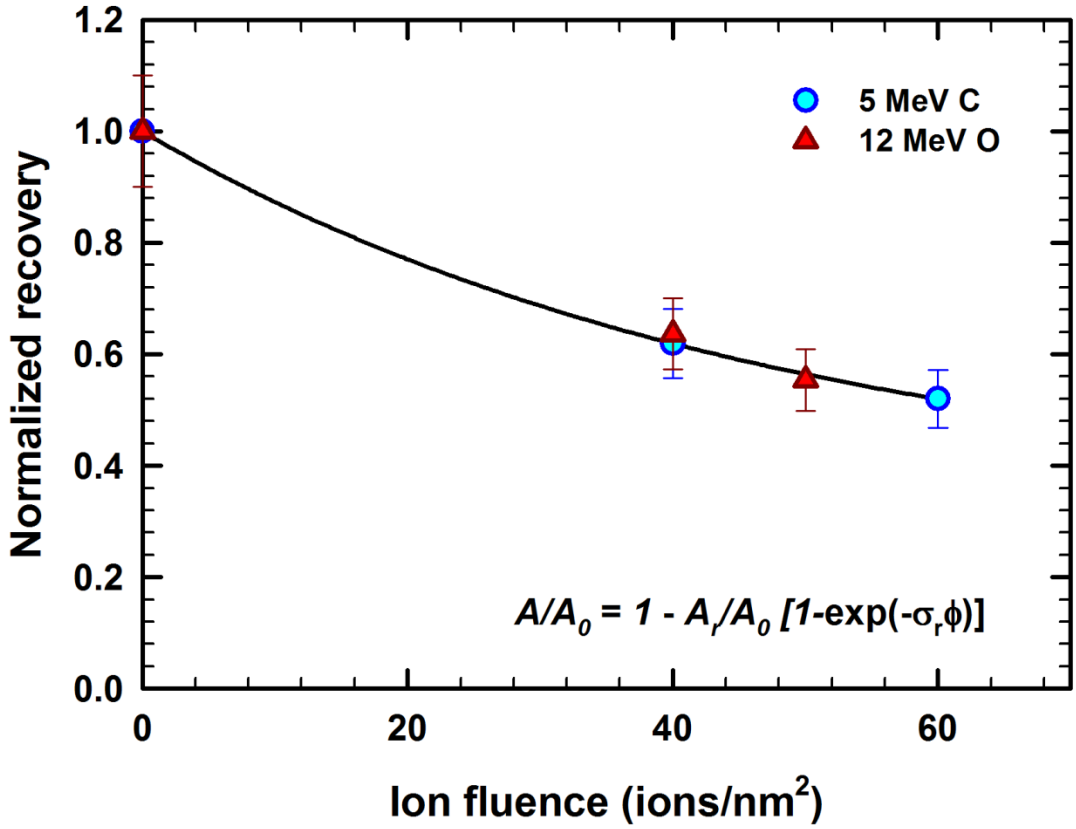

Fig. 3. Dependence of the normalized recovery vs. ion fluence for C (filled circle) and O (filled triangles) irradiation. Solid curve is a fit of Eq. (2) to the experimental results.

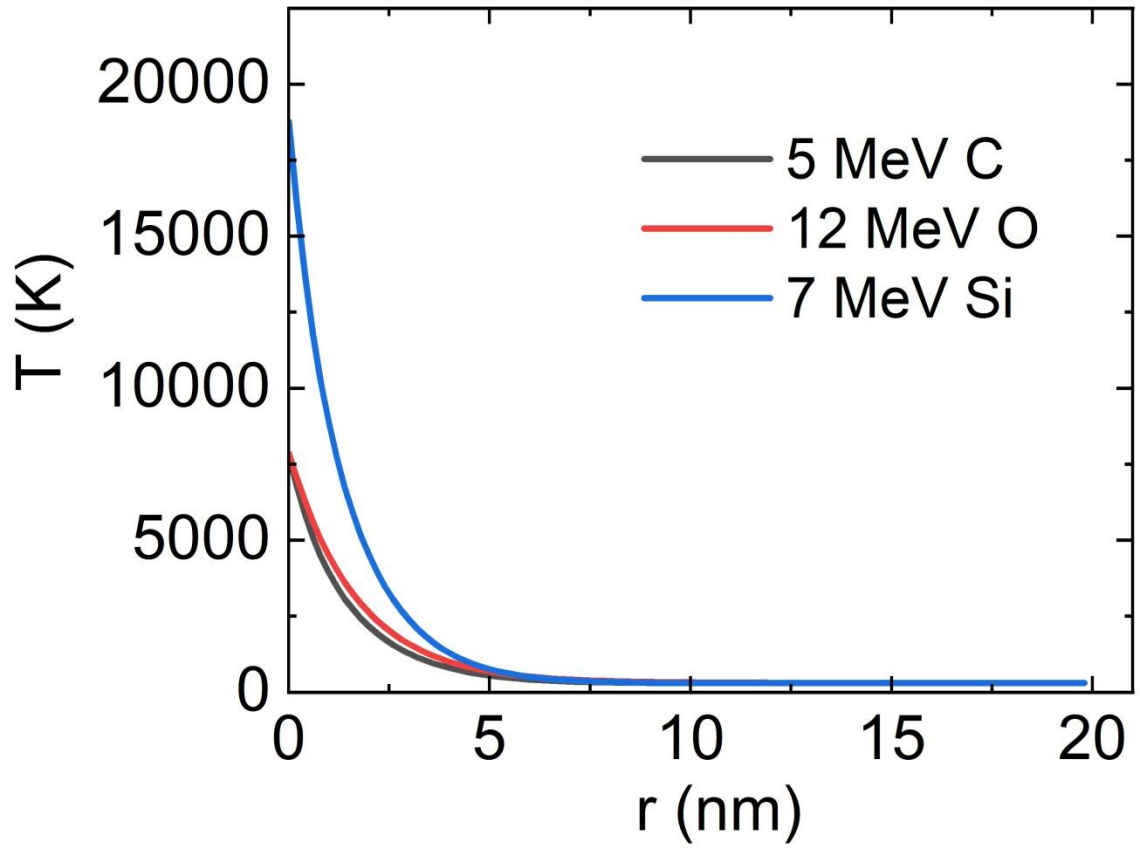

Fig. 4. The radial profile of maximum lattice temperature in defective KTaO3 predicted at a time of 30 fs by the 2T-MD for the indicated ion species.

Revealing two-stage phase transition process in defective $KTaO_3$ under inelastic interactions

D. Iancu[a,d], E. Zarkadoula[b], M. D. Mihai[a], C. Burducea[a], I. Burducea[a], M. Straticiuc[a], Y. Zhang[b,c], W. J. Weber[c**] and G. Velişa[a*]

[a]Horia Hulubei National Institute for Physics and Nuclear Engineering, Măgurele, IF 077125, Romania
[b]Materials Science and Technology Division, Oak Ridge National Laboratory, Oak Ridge, TN 37831, USA
[c]Department of Materials Science & Engineering, University of Tennessee, Knoxville, TN 37996, USA
[d]University of Bucharest, Faculty of Physics, Măgurele, IF 077125, Romania

Modeling details

As an energetic charged particle penetrates a material, it transfers energy to both atomic nuclei and electrons in the material. Initial atomic displacement events occur with target nuclei that create an assortment of defects, such as vacancies, interstitials, and small defect clusters, but keeps the atomic structure largely intact. Moreover, much of the electronic energy eventually dissipated to atomic lattice can lead to highly-local inelastic thermal (transient) spikes that induce athermal atomic mobility and defect recovery. The molecular dynamics (MD) simulations were executed using the DL_POLY MD package [1]. An empirical interatomic potential [2] was used to describe the system, which was joined to short-range Ziegler–Biersack–Littmark (ZBL) repulsive potentials [3] to account for the strong repulsive interactions of energetic recoiling atoms at short interatomic distances. The systems employed consist of about 320,000 atoms and have periodic boundaries. 30% Frenkel pairs were randomly produced in the system, to correspond to disorder level on 0.30, as described in our previous work [4]. Each system was equilibrated using the constant temperature and pressure ensemble (NPT) prior to each irradiation simulation. For each system, a transient thermal spike was applied to the system along the z-direction of the MD box. The MD simulation of each thermal spike was performed using the microcanonical ensemble (NVE), using an adaptive time-step. A Langevin thermostat with a width of 10 Å was applied along the x- and y- dimensions of the

system to model the energy dissipation in the bulk. The defects before and after the thermal spike simulations were identified using the sphere criterion with a cut-off radius of 0.75 Å [5]. The irradiation simulation was run for 50,000 steps (about 75 ps). Overall, the interatomic potential used in this work, while not fitted to non-equilibrium processes, has provided good agreement with the experimental results here and in previous work [4,6,7], providing useful insights into the lattice response due to swift ion irradiation, both in pristine and pre-damaged systems.

RBS/C results

Fig. S1 shows that Au ion irradiations to ion fluences of 0.11 ions/nm^2 (see black lines in Fig.1 (a-c)) has induced an initial maximum level of fraction disorder (f_0) of 0.35 on the Ta sublattice. Sequential irradiation with 5 MeV C ions to an ion fluence of 10 ions/nm^2 induces an increase in peak level of disorder ($f^* \sim 0.47$). This peak level of disorder exhibits a systematic decrease with continued irradiation to ion fluences from 10 to 30 ions/nm^2 and then to 80 ions/nm^2, which is similar to that observed for a higher initial level of disorder (Fig. 2). The reduction of the amount of disorder at the damage peak at higher fluences is accompanied by some broadening of the disorder profiles with increasing C fluence [8]. In addition to thermal spike annealing, as discussed in the main article, enhanced defect mobility due to electronic excitations may also be active, as experimentally evidenced by the broadening of the damage profile for C ions at the highest fluence. Intense ionization and electronic excitations, for which energy dissipation processes are impacted by the local atomic arrangement, can lead to nonequilibrium athermal processes, reduce energy barriers and encourage strain relaxation, defect diffusion, defect recovery, and even amorphous-to-crystalline phase transformations [11]. Such athermal processes are normally temperature independent with much reduced activation energies. In other words, defect diffusion and recovery are enhanced under electronic excitation processes (ionization-enhanced diffusion).

In the case of O ions (Fig. 1(b)), ionization-induced recovery occurs without any increase in disorder, perhaps due to the slightly smaller value of S_n. In addition, the damage recovery and defect migration is more pronounced than in the case of C ions, due to the higher S_e for 12 MeV O, leading to higher temperature thermal spikes and enhanced defect mobility, both of which increase the efficiency of recovery [8]. It should be emphasized that irradiation-induced disorder from 7 MeV Si ions is not observed in the virgin crystal (Fig. S1(c)), at least up 0.2 ions/nm^2; on the other hand, for the C and O ion irradiations of virgin $KTaO_3$, there is clear experimental evidence of damage production at much higher fluences from the RBS/C measurements (Fig. S1(c)). One needs to keep in mind that the C and O ion fluences, at which discernible disorder in virgin $KTaO_3$ is detectable by RBS/C, are 100 times higher than the ion fluence used for Si. Ion channeling analyses of 18 MeV Ni [4], 358 MeV Ni [9] and 91.6 MeV Xe [4] irradiated virgin $KTaO_3$ have confirmed that ion tracks are produced in virgin $KTaO_3$ only for S_e values above 10.81 keV/nm, which is significantly higher than the S_e values for both C and O ions used in the current study. Consequently, under these conditions the formation of ion tracks is not expected; however, some displacement damage associated with energy dissipation from S_e [8] or S_n (or both) is likely generated along the ion trajectories via interstitial ejection from the thermal spike, bond breakage due to local electronic excitations, or elastic collision processes. A similar effect has been observed for other pristine materials (e.g., GaAs and InP) irradiated with ionizing ions having S_e values below S_e^{th}, which resulted in the generation of only point defects and point defect complexes [10,11]. Unfortunately, once the ion fluence of C and O ions exceeded 25 ions/nm^2, both virgin and pre-damaged $KTaO_3$ samples start to exhibit some microcracking on the surface that increased with increasing ion fluence, as shown by the AFM results in Fig. S2. Similar crack formation has been reported in defective $KTaO_3$, which was subsequently irradiated with 91.6 MeV Xe ions to 0.01 ions/nm^2, and has been attributed to macroscopic swelling caused by

amorphous tracks or stress relaxation near the crystal surface that is generated by the irradiation-induced phase modification [4]. Since no amorphous tracks are expected to form under these conditions, the observed microcracks are attributed to the volumetric swelling generated by the irradiation-induced amorphous transition that occurs at the end of range for the 5 MeV C and 12 MeV O ions, as previously observed in virgin SiC simultaneously irradiated at 300 K with 900 keV I and 36 MeV W ions [12].

Atomic force microscopy (AFM) results

Atomic force microscopy (AFM) micrograph recorded on virgin $KTaO_3$ irradiated with 12 MeV O ions at a fluence of 50 ions/nm^2 depicts the formation of cracks, as shown in Fig. S2(a). As shown in Fig. S2(b), profilometry of the crystal surface across one crack demonstrates that these cracks (~1500 nm in depth) are much deeper than the region where pre-existing defects exist (first 500 nm of the matrix).

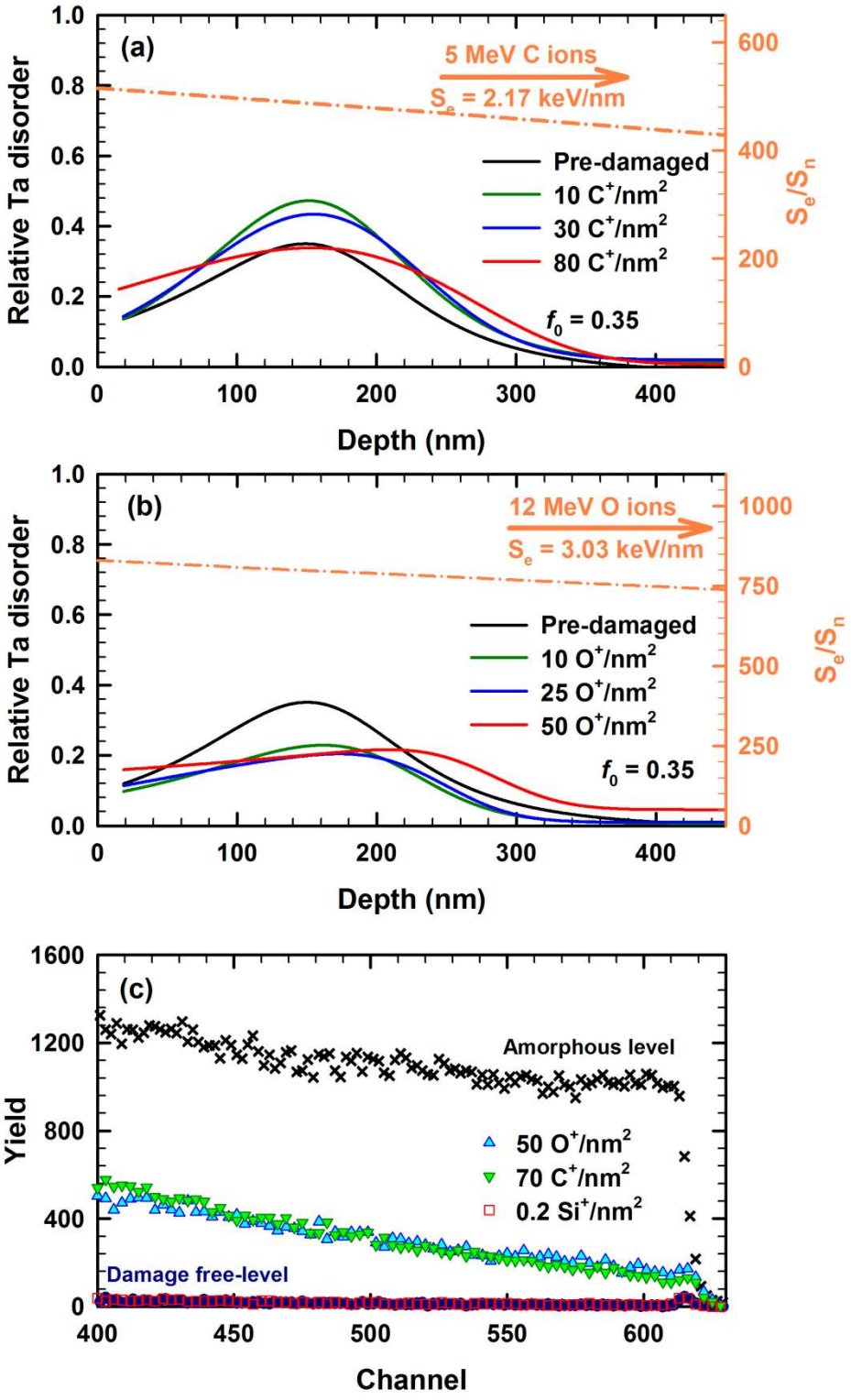

Fig. S1. Relative Ta disorder profiles for pre-damaged $KTaO_3$ with a maximum initial disorder fraction f_0 = 0.3 and subsequently irradiated with: (a) C ions and (b) O ions. Note that the parameters (ion energy, fluence and S_e) are indicated in the figure. Also superimposed are the SRIM-derived S_e/S_n ratios (dash lines). The RBS/C spectra recorded for virgin $KTaO_3$ irradiated with 5 MeV C, 7 MeV Si and 12 MeV O ion irradiations at the indicated fluences are shown in (c) together with the RBS spectra recorded in random and channeling direction from a pristine crystal.

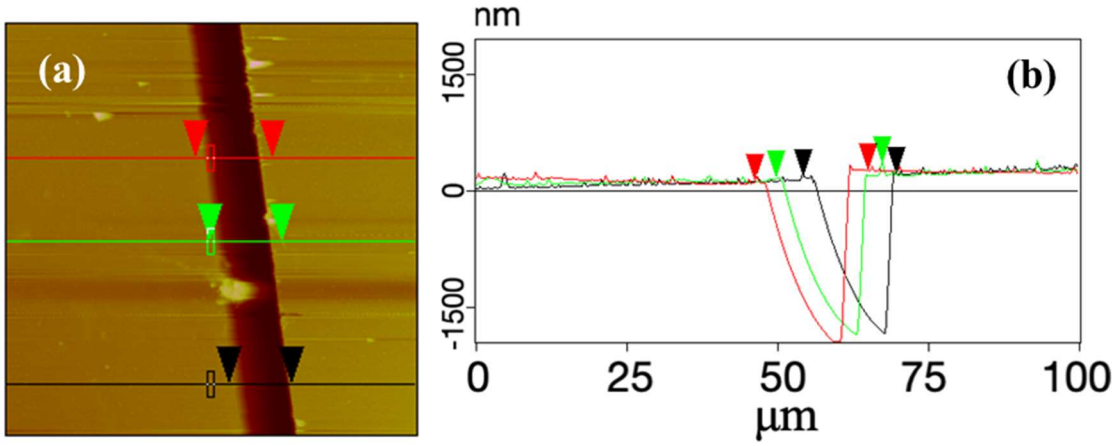

Fig. S2. (a) AFM micrograph recorded on virgin $KTaO_3$ irradiated with 12 MeV O ions at a fluence of 50 ions/nm^2. (b) Depth of crack measured by profilometry at different positions along the crack shown in (a).

References

[1] I.T. Todorov, W. Smith, K. Trachenko, M.T. Dove, DL_POLY_3: New dimensions in molecular dynamics simulations via massive parallelism, J. Mater. Chem. 16 (2006) 1911–1918. doi:10.1039/b517931a.

[2] J.F. Ziegler, J.P. Biersack, The Stopping and Range of Ions in Matter, in: Treatise Heavy-Ion Sci., Springer US, Boston, MA, 1985: pp. 93–129. doi:10.1007/978-1-4615-8103-1_3.

[3] M.A. McCoy, R.W. Grimes, W.E. Lee, Phase stability and interfacial structures in the Sr0-$SrTiO_3$ system, Philos. Mag. A Phys. Condens. Matter, Struct. Defects Mech. Prop. 75 (1997) 833–846. doi:10.1080/01418619708207205.

[4] G. Velişa, E. Zarkadoula, D. Iancu, M.D. Mihai, C. Grygiel, I. Monnet, B. Kombaiah, Y. Zhang, W.J. Weber, Near-surface modification of defective $KTaO_3$ by ionizing ion irradiation, J. Phys. D. Appl. Phys. 54 (2021) 375302. doi:10.1088/1361-6463/AC0B11.

[5] T. I. T. Todorov and W. Smith, No Title, He DL Poly 4 User Manual, v. 4, Www.Ccp5. (2012)., Ac.Uk/DL_POLY/MANUALS/USRMAN4.Pdf. (n.d.).

[6] E. Zarkadoula, K. Jin, Y. Zhang, W.J. Weber, Synergistic effects of nuclear and electronic energy loss in $KTaO_3$ under ion irradiation, AIP Adv. 7 (2017) 1–8. doi:10.1063/1.4973938.

[7] E. Zarkadoula, Y. Zhang, W.J. Weber, Molecular dynamics simulations of the response of pre-damaged $SrTiO_3$ and $KTaO_3$ to fast heavy ions, AIP Adv. 10 (2020) 015019. doi:10.1063/1.5133061.

[8] W.J. Weber, H. Xue, E. Zarkadoula, Y. Zhang, Two regimes of ionization-induced recovery in $SrTiO_3$ under irradiation, Scr. Mater. 173 (2019) 154–157. doi:10.1016/J.SCRIPTAMAT.2019.08.013.

[9] X. Han, Y. Liu, Q. Huang, M.L. Crespillo, P. Liu, X. Wang, Swift heavy ion tracks in alkali tantalate crystals: a combined experimental and computational study, J. Phys. D. Appl. Phys. 53 (2020) 105304. doi:10.1088/1361-6463/AB5EE6.

[10] E. Wendler, B. Breeger, C. Schubert, W. Wesch, Comparative study of damage production in ion implanted III–V-compounds at temperatures from 20 to 420 K, Nucl. Instruments Methods Phys. Res. Sect. B Beam Interact. with Mater. Atoms. 147 (1999) 155–165. doi:10.1016/S0168-583X(98)00597-7.

[11] W. Wesch, A. Kamarou, E. Wendler, Effect of high electronic energy deposition in semiconductors, Nucl. Instruments Methods Phys. Res. Sect. B Beam Interact. with Mater. Atoms. 225 (2004) 111–128. doi:10.1016/j.nimb.2004.04.188.

[12] L. Thomé, G. Velisa, S. Miro, A. Debelle, F. Garrido, G. Sattonnay, S. Mylonas, P. Trocellier, Y. Serruys, Recovery effects due to the interaction between nuclear and electronic energy losses in SiC irradiated a dual-ion beam, J. Appl. Phys. 117 (2015) 105901. doi:10.1063/1.4914305.